



# Forming dependence on spin roller paths for thin-walled complex components from 2195 Al-Li alloy TWBs

Hongrui Zhang<sup>1,2,3</sup> · Mei Zhan<sup>1,3</sup> · Zebang Zheng<sup>1,2,3</sup> · Rui Li<sup>1,3</sup> · Fei Ma<sup>4</sup> · Xiaolei Cui<sup>1,3</sup> · Shuwan Chen<sup>1,3</sup> · Yudong Lei<sup>1,3</sup>

Received: 9 October 2021 / Accepted: 24 February 2022 / Published online: 1 March 2022  
© The Author(s), under exclusive licence to Springer-Verlag London Ltd., part of Springer Nature 2022

## Abstract

The spin forming provides an approach to manufacturing large-diameter thin-walled complex curved surface components based on tailor-welded blanks produced from small 2195 Al-Li alloy plates, even scraps by friction stir welding (FSW). In this study, three spin forming schemes of single-pass, two-pass, and three-pass roller paths are designed. The corresponding experimental results indicate that the rolling of the rollers during spin forming is helpful in reducing the wall thickness inhomogeneity between weld and parent material and hence improves the surface roughness. Meanwhile, spin forming makes the welds deflect. With the increase of spinning passes, the forming height, open diameter, and the weld deflection angle of components increase. Additionally, the wall thickness difference, the surface quality, and the overall unfitability of components are all improved to some extent. However, there still exists insufficient forming height and over large open diameter due to the unfitability. Therefore, to obtain an ideal formed component, a spin forming scheme was proposed through increasing spinning passes in the ellipsoidal and cylindrical segments of the mandrel. Using this improved scheme, the forming height was increased with the maximum of 18%, the unfitability value was decreased with the maximum of 97%, the surface quality was significantly improved, and the ideal spun component was obtained.

**Keywords** Spin forming · Friction stir welding · Thin-walled component · Roller path · Tailor welded blank

## 1 Introduction

Thin-walled complex curved surface components are widely used in advanced aircraft, spacecraft, etc., to reduce the total weight and increase the thrust-to-weight ratio of the

engine. A typical representative is the 2195 Al-Li special curved surface heads in the aerospace industry. These components can be effectively manufactured using spin forming, owing to the advantages of high process flexibility, outstanding mechanical property, small forming loads, and low manufacturing cost [1, 2]. With the improvement of the carrying capacity of aerospace equipment, thin-walled complex curved surface components with larger diameters are urgently needed, such as 10 m. However, large diameter components are difficult to be manufactured using the traditional single integrated blanks due to the limitation of the production capacity of ultra-wide sheets. A hybrid manufacturing technology exploiting friction stir welding (FSW) followed by spin forming has been proposed to overcome this issue. In addition, using the FSW technique to produce tailor welded blanks (TWBs) can make use of small sheet metal blanks or scraps, which contributes to green sustainable development [3].

It is well-known that the spin formability of thin-walled curved surface components is significantly affected by multiple forming factors, including roller paths. To develop an efficient spin forming process, many scholars have studied

✉ Mei Zhan  
zhanmei@nwpu.edu.cn

✉ Zebang Zheng  
zebang.zheng@nwpu.edu.cn

<sup>1</sup> Shaanxi Key Laboratory of High Performance Precision Forming Technology and Equipment, School of Materials Science and Engineering, Northwestern Polytechnical University, Xi'an 710072, China

<sup>2</sup> Key Laboratory of High Performance Manufacturing for Aero Engine (Ministry of Industry and Information Technology), School of Mechanical Engineering, Northwestern Polytechnical University, Xi'an 710072, China

<sup>3</sup> State Key Laboratory of Solidification Processing, School of Materials Science and Engineering, Northwestern Polytechnical University, Xi'an 710072, China

<sup>4</sup> Sichuan Aerospace Long March Equipment Manufacturing Co., Ltd, Chengdu 610100, China

the effects of the roller path on the spin forming of components. Wang and Long [4] established a finite element (FE) model of spinning for thin-walled components with curved surfaces to investigate the effects of the roller path profile on component wall thickness. The results indicated that the concave path caused the highest tool forces and wall thickness reductions. Mohebbi and Rahimi Pour [5] studied the influence of linear and nonlinear paths on spin forming from a blank to a tubular shape, and the results showed that the nonlinear path of the roller failed to produce this tubular component and easily caused circumferential cracks. Wu et al. [6, 7] indicated that the gap was the most important parameter for the spin forming of the large-sized cone and it was concluded that the forming height first increased and then decreased with the increase of gap. For spin forming quality, different roller path types, including line, arc, and involute in multi-pass conventional spinning, were studied by Wei et al. [8] and Su and Wei [9] and found that the involute roller path is the best. Gan et al. [10, 11] studied the effect of roller paths based on quadratic Bezier curves on forming quality during multi-pass conventional spin of hemispherical components. It was found that the first roller path had a significant effect on wall thickness distribution, and the backward pass can obviously improve the uniformity of wall thickness. Li et al. [12] found that in the die-less spinning of sheet metal, a combined roller path with a convex-concave curve could contribute a low shape deviation, while an inverse combined roller path gives better thickness precision.

In addition to the above research on the roller path of the spin forming of single integral blanks, many researchers have paid more attention to the plastic forming of tailor welded blanks. Katiyar et al. [13] developed an FE model to predict the complex crushing behavior of stretch-formed domes. Liu et al. [14] revealed the deformation behavior and failure feature with TWBs manufactured by varying thickness blanks in the hemispherical punch stretching test. In order to achieve the failure/necking features of TWBs, a forming limit prediction model was proposed. Parente et al. [15] performed an experimental study on TWBs produced by FSW with dissimilar aluminum alloy thin sheets and pointed out that TWB formability is highly dependent on weld line orientation. Based on numerical simulations, Kinsey et al. [16] introduced a TWB deep drawing process with a geometry similar to that of an inner door and indicated the effectiveness and feasibility of the TWBs forming technology. Khan et al. [17] studied the effect of the aspect ratio on formability characteristics of TWBs and found that the weld line displacement tends to increase with the increasing of the TWBs thickness ratio. Zadpoor et al. [18] studied the effects of the thickness difference and machining on

the mechanical behavior of machined aluminum TWBs by experimental and numerical methods. They pointed out that the machining process and thickness difference significantly affected the forming behavior and failure mechanism of the specimens. Silva et al. [19] performed the single point incremental forming of TWBs produced by FSW and concluded that the single point incremental forming with TWBs is prospective for manufacturing complex metal components. To minimize the movement of the weld line of TWBs, Bhagwan et al. [20] studied the weld movement of TWBs. The results indicated that the reduction in weld shift obtained by replacing the thick blank with lower strength alloys is substantial at lower gage mismatch ratios. Moayedi et al. [21] studied the effects of weld orientation on the formability of TWBs and suggested that TWB with orientation weld  $90^\circ$  in tension mode could achieve the best formability while in-plane strain condition; the best formability is originated from TWB with weld orientation  $0^\circ$ .

The achievements in the aforementioned literature strongly contribute to the spin forming with single integral blanks for thin-walled curved surface components and the common plastic forming with TWBs. Furthermore, in order to form large-size thin-walled complex curved surface components, the combined manufacturing process of stamping and tailoring welding has always been the currently common practice. However, this combined manufacturing method leads to high cost, inefficient manufacturing practices, high failure risk, low shape precision, and large residual stress. Hence, in order to realize the manufacturing of large diameter components and reusing of industrial metal scraps, it is necessary to develop TWBs spin forming for thin-walled complex curved surface components.

For this purpose, in this study, three spin forming schemes of single-pass, two-pass, and three-pass roller paths for 2195 Al-Li alloy thin-walled complex curved surface components are proposed, and the forming experiments are conducted. It is concluded that the rolling of rollers is benefit to reduce the wall thickness difference between the weld and parent material resulting from FSW and then to improve the surface roughness of the weld zone and wall thickness homogeneity. However, the shape and size cannot meet the requirements due to the unfitability of these components. On this basis, an improved spin roller path scheme for thin-walled complex curved surface components is proposed. Finally, through the spin forming scheme, the forming quality of spun components was significantly improved. The research provides a basis and guidance for forming process design and tailoring of product quality in spinning of 2195 Al-Li alloy thin-walled complex curved surface components.

## 2 Research methodology

### 2.1 Hybrid forming strategy

The hybrid forming strategy integrating friction stir welding and spin forming used in this study is shown in Fig. 1. This forming strategy provides a novel potential approach to manufacturing large diameter thin-walled complex curved surface components. The diameter of target components is generally larger than 3 m. In this study, for the purpose of exploring the feasibility of this forming strategy and reducing material consumption, the spinning experiments were carried out on a small-scale component. The material used in this study is a commercial rolled and annealed 2195 Al-Li alloy blanks with a thickness of 3 mm. Two blanks of identical size were first friction stir welded to form a tailor welded blank, and the welding process parameters are shown in Table 1. The mechanical property parameters of the parent material and weld of TWBs are listed in Table 2. The TWB was then tailored into a round shape with a diameter of 370 mm. Next, the welding burrs and flash are removed using a grinding machine to avoid scratching the blank surface during the spinning. Finally, the thin-walled complex curved surface components are manufactured through spin forming.

The spin forming experiments were conducted on a computer numerical control (CNC) spin forming machine PS-CNC SX Y1500HD with two symmetrically distributed rollers rotating freely around their axis. The schematic diagram of the spin setup and the geometries of the mandrel and rollers are shown in Fig. 2. In this study, the shape of the spun experimental components is consistent with the shape of the spinning mandrel. The ideal height and open-end

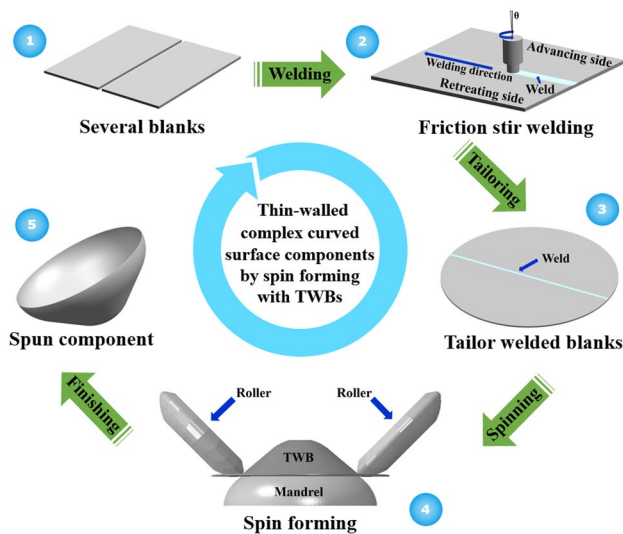


Fig. 1 Flow chart of the hybrid manufacturing strategy

Table 1 Process parameters of friction stir welding

Welding parameter	Value
Welding feed speed (mm/min)	150
Tool rotational speed (rpm)	800
Plunge depth (mm)	0.1
Shoulder diameter (mm)	10
Pin length (mm)	2.8

diameter of spun experimental components are 143 mm and 333.8 mm, respectively. In particular, the surface profile of the mandrel consists of four different parts: arc segment (A), cone segment (B), ellipsoid segment (C), and cylindrical segment (D). During spinning, the surfaces of the mandrel, rollers, and TWBs are all coated with drawing oil to improve lubrication conditions.

### 2.2 Spin roller paths design of TWBs

In order to explore the best processing route for the thin-walled complex curved surface component, three TWB spin forming schemes are designed, as shown in Fig. 3. These schemes are composed of single-pass, two-pass, and three-pass spin roller paths, respectively. For the single-pass spin forming scheme, the roller path is designed to be the same as the mandrel generatrix shape (Fig. 3a). Since the half cone angle of the cone segment is 50°, the two-pass spin forming scheme, as shown in Fig. 3b, was designed by adding a cone spinning path with a half-cone angle of 50° based on the single-pass scheme. Likewise, the three-pass spin forming scheme in Fig. 3c is formed by adding another cone spinning path with a half-cone angle of 76° based on the two-pass scheme. The additional spinning path follows the tangent of the arc segment of the mandrel. The common spin forming parameters of these schemes are summarized in Table 3.

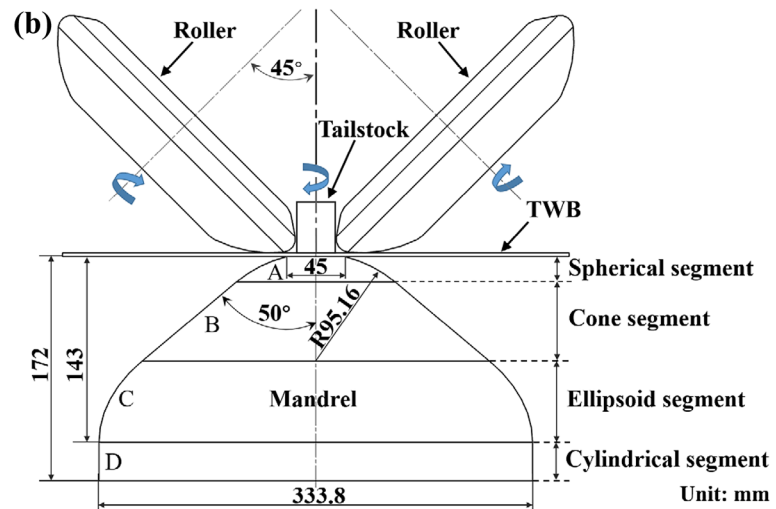
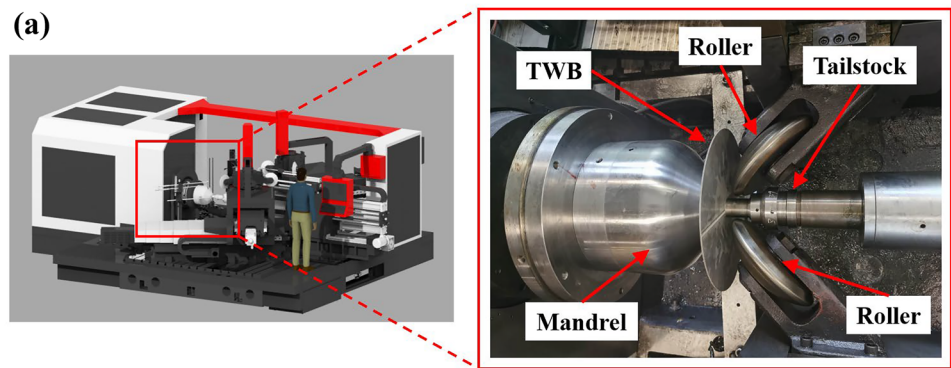
### 2.3 Index and measurement

To study the effects of different spin forming path designs on forming quality of spun components, the geometries (forming height, forming diameter, wall thickness distribution, unfitability distribution) and the surface roughness

Table 2 Mechanical property parameters of 2195-O Al-Li alloy TWBs

Parameters	Values	
	Parent material	Weld
Young’s modulus/GPa	73	79
Yield strength/MPa	122.7	129
Tensile strength/MPa	181	215

**Fig. 2** Experimental equipment: **a** CNC spin forming machine and **b** schematic diagram of spin setup



were used as evaluation indexes. The geometry indexes can be obtained by a handheld three-dimensional laser scanner based on reverse engineering. It is considered to be ideal if the forming height is more than 143 mm, namely,

the spun components are spun to the cylindrical segment of the mandrel. In addition, the unfitability distribution of spun components was achieved through the schematic views of assembly drawings of spun components and the

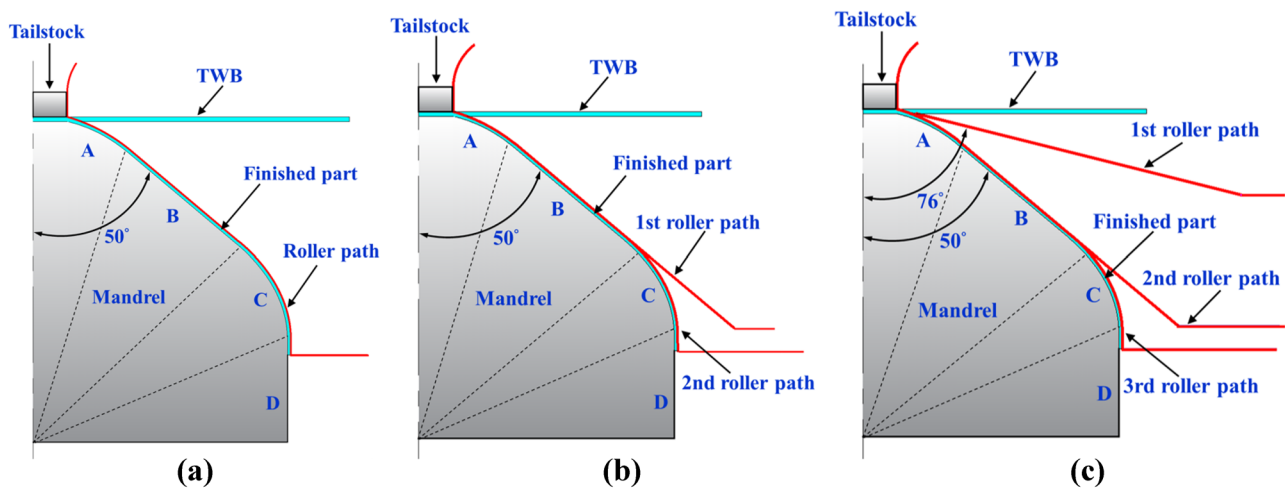


**Fig. 3** Schematic illustration of TWB spin forming schemes: **a** single-pass, **b** two-pass, and **c** three-pass

**Table 3** Process parameters of TWBs spin forming

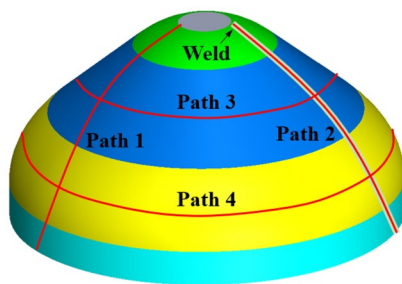
Spin forming parameters	Value
Roller operating angle (°)	45
Roller nose radius (mm)	10
Mandrel rotational speed (rpm)	200
Roller feed speed (mm/min)	400
Lubrication condition	Drawing oil

mandrel. In order to analyze the unfitability of experimental components, a measurement method is developed to quantify the unfitability that at the same section height of components and mandrel, the distance between the inner surface of components and the mandrel surface is used as the evaluation index of the unfitability. To ensure accuracy, this distance  $U$  is measured five times and averaged by selecting six evenly distributed positions on the open-end of each component. Accordingly, the measure  $U$  is defined as follows:

$$U = \frac{1}{n} \sum_{i=1}^n (R_{S_i} - R_{M_i}) \quad (1)$$

where  $n=6$  is the measurement times;  $R_{S_i}$  and  $R_{M_i}$  are the distance from the inner surface of components and mandrel surface to the central axis of the mandrel, respectively.

In addition, the wall thickness was measured by this reverse engineering. To obtain the axial wall thickness distributions of components in weld and parent material, two measuring paths in the parent material zone (Path 1) and weld zone (Path 2) along the axial direction of the spun component were selected respectively. And the two circumferential paths at the cone segment (Path 3) and ellipsoid segment (Path 4) of spun components were selected, respectively, as shown in Fig. 4. Besides, in this study, the surface quality of spun components under three spin roller path schemes was obtained using a three-dimensional high-resolution optical surface measuring instrument.

**Fig. 4** Schematic diagram of measure paths for the thickness analysis

### 3 Results and discussion

According to the roller path schemes, the spin experiments of TWBs were carried out. The forming results in geometry and surface qualities of formed components were analyzed in this section.

#### 3.1 Height and diameter

The heights and open-end diameters of spun components under the three roller paths are obtained, as shown in Fig. 5. It shows that the height increases from 123.7 to 132 mm, and the diameter increases from 336.6 to 339.2 mm with the increase in spinning pass. This is mainly because that there are more material which was rolled and deformed under the roller action with the increase in spinning pass. Even though the height still not reaches the ideal value, the diameter increases to a larger value than the ideal diameter.

Figure 6 shows that the unfitability value of spun components decreases from 3.4 to 2.0 mm then increases to 2.3 mm, as increasing spinning path. The over large diameter is mainly due to the unfitability caused by springback, particularly in the ellipsoid segment. In addition, it can also be found from Fig. 6 that the unfitability distribution under the single-pass scheme occurred in the ellipsoid segment. While it was clearly seen in Fig. 6, the unfitability distribution zone increased significantly under the two-pass and three-pass schemes and mainly occurred in the cone segment and the ellipsoid segment.

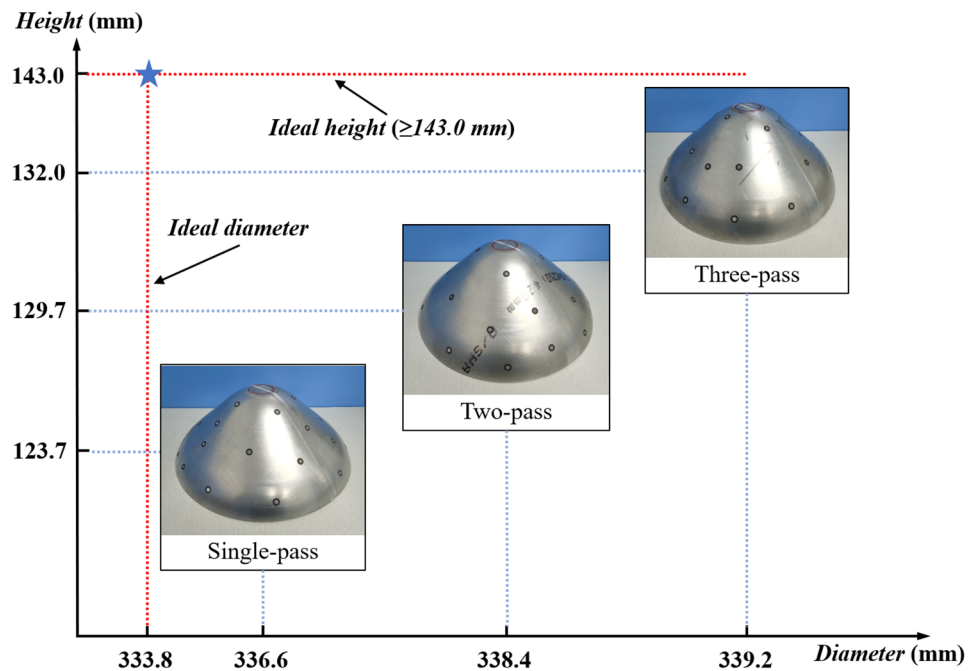
#### 3.2 Wall thickness

The axial and circumferential wall thickness distributions of spun components in the weld zone and parent material zone under three spin roller path schemes are shown in Fig. 7. It can be seen that the values of wall thickness in weld under a given roller path are generally smaller than the corresponding values in the parent material. These are mainly because of the weld thinning caused by the FSW process. In addition, with the increase of spinning passes, the variation trend of wall thickness tends to be consistent. The average differences in axial and circumferential wall thickness between parent material and weld were the smallest when the three-pass spin roller path scheme was conducted. These indicated that the wall thickness homogeneity is improved by spinning and the increase of spin passes.

#### 3.3 Weld torsion

After spin forming of TWBs, an obvious deflection phenomenon occurred at the welds of spun components, as shown in Fig. 8a. From Fig. 8b, it can be observed that the weld

**Fig. 5** Heights and diameters of components under three spin roller paths



deflection direction is in accordance with the rotating direction of spun components. During spinning, with the forward feed of the roller along the axial direction of the mandrel, the welds of spun components present deflection. Although Ma et al. [22] have also studied the spin forming of the curved head with a 2219 aluminum alloy TWB, the weld deflection of the curved head did not occur after spinning. This is because there is not enough material flow under fewer spinning passes. In the present study, it can be concluded according to the maximum weld deflection angle (Fig. 8b)

that accompanied by the increase of spin passes of TWBs, the weld deflection angle increases gradually under roller rolling.

### 3.4 Surface quality

Figure 9 shows the surface roughness parameter  $R_a$  in the parent material and weld zone of spun components under three spin forming path schemes. It can be concluded that with the increase of spin passes, the surface roughness values in the parent material and weld zone are all gradually decreased, and the surface roughnesses along the latitude direction of spun components are better than those along the longitude direction of spun components. In addition, as compared to the obvious onion rings in the weld thinning zone of the original TWB, the onion rings in the weld thinning zone are gradually eliminated by roller rolling with the increase of spin passes, as shown in Fig. 9. The main reason is that with the increase of spin passes, the increased roller rolling on the material contributes to the improvement of the surface roughness.

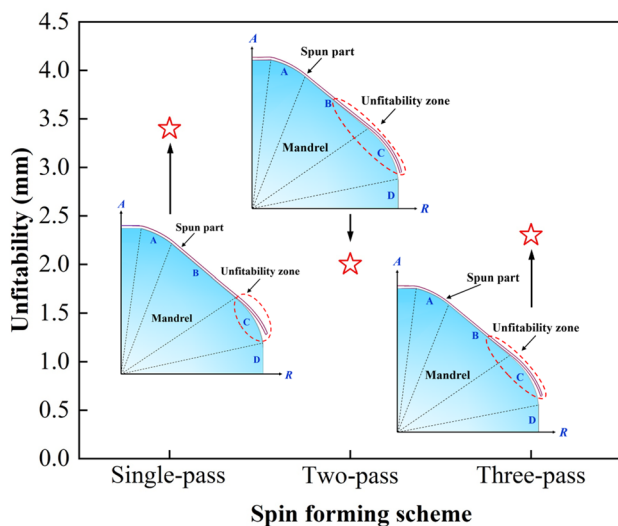


**Fig. 6** Unfitability of spun components under three spin roller paths

## 4 Improvement on spin roller paths

According to Sect. 3, the increase of spin passes is beneficial to improve the forming height and decrease the unfiability so as to obtain spun components with better forming quality. Since the unfiability distribution of spun components mainly focuses on the ellipsoid segment, therefore, the three spin forming schemes in Sect. 2.2 are tailored and tried by

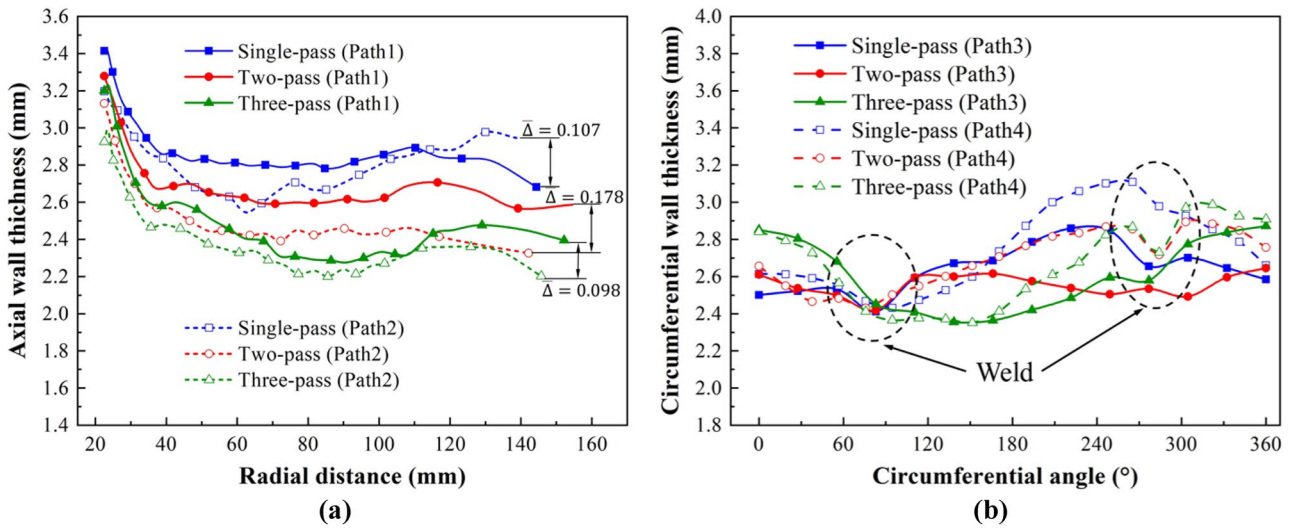


Fig. 7 Axial and circumferential wall thickness distributions of spun components under three spin roller path schemes

Fig. 8 Weld deflection of spun components under a given three-pass spin roller path scheme (a) and under various spin roller path schemes (b)

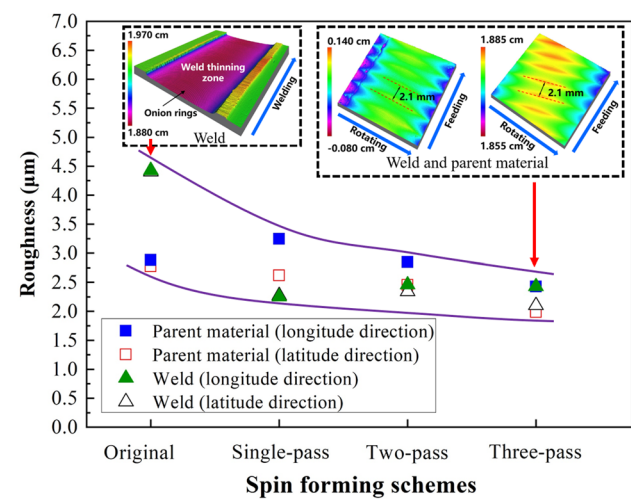
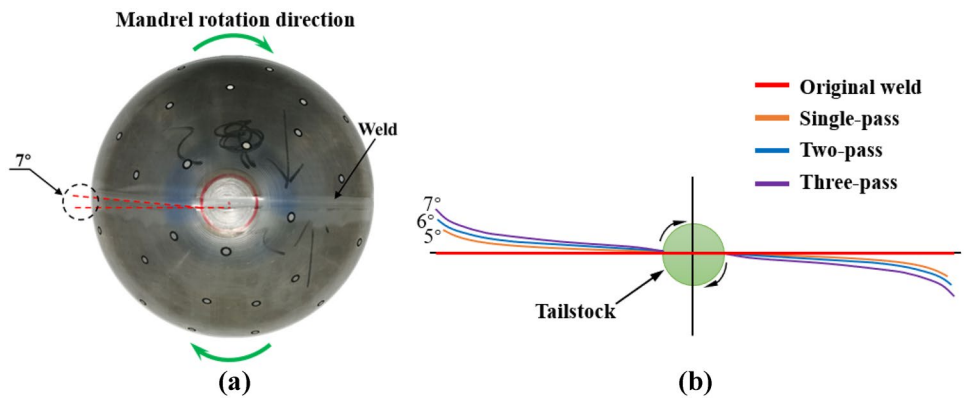


Fig. 9 Surface roughness of spun components under three spin roller path schemes

adding a spinning pass along the generatrix of the mandrel. The results of the unfitability are summarized in Table 4. Obviously, despite adding a spinning pass, the unfitability is still not decreased but increased and compared with before tailoring, the unfitability distribution increased. Therefore, according to the above process tries, it is not advisable to simply increase the number of spinning passes. From the previous experimental analysis results, it is found that the unfitability distribution is mainly concentrated in the ellipsoid segment. As a consequence, the improved spin roller path scheme is proposed by adding seven spin passes at the ellipsoid segment and cylindrical segment of the mandrel on the basis of the single-pass spin roller path scheme. Namely, an eight-pass spin roller path scheme was proposed, as shown in Fig. 10.

Exploiting this proposed eight-pass spin roller path scheme, the spun experimental component with the forming height of 145.7 mm and open diameter of 333.8 mm was obtained, as shown in Fig. 11. Comparing Figs. 7 and

**Table 4** Unfitability comparison of spun components after adding one pass

Original roller path scheme	Tailored scheme by adding one pass	Unfitability value (mm)	Unfitability trend
Single-pass	Two-pass	3.4→3.9	↑
Two-pass	Three-pass	2.0→2.58	↑
Three-pass	Four-pass	2.3→2.45	↑

12, it can be seen that under this eight-pass spin roller path scheme, the inhomogeneous circumferential wall thickness distribution is significantly improved, and the differences in the circumferential wall thickness between parent material and weld are greatly reduced. Likewise, a weld deflection of 10° occurred under this spin roller path scheme, which indicates that the weld deflection angle increases with the increase of spin passes. The forming results of spun components under four spin roller path schemes are listed in Table 5. It can be found that using the improved eight-pass spin forming scheme, the forming height of spun components is highest, and there is a maximum increase of 18% on forming height. In addition, from Table 5, the unfitability value of spun components is only 0.09 mm and compared with components under single-pass spin forming schemes, the maximum decline of the unfitability value is 97%. That is to say, using the proposed eight-pass spin roller path scheme, the profile shape of spun components is in good agreement with the mandrel. Besides, it can also be clearly seen from Table 5 that the



**Fig. 11** Spun component under the eight-pass spin roller path scheme

spacings of the spinning corrugations are decreased from 2.3 to 1.2 mm, and as shown in Fig. 13, the onion rings in the weld zone are absolutely eliminated by roller rolling. It can be concluded that the surface roughness values are also better not only in the weld zone but also in the parent material zone using the proposed eight-pass spin forming scheme. Therefore, there is no doubt that using the proposed eight-pass spin forming scheme can effectively avoid the above forming quality problems, improve the spin forming quality significantly, and obtain the ideal spun components.

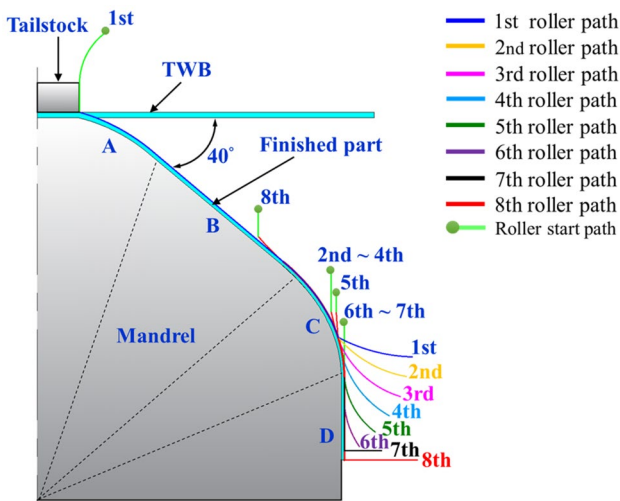


**Fig. 10** Schematic illustration of the eight-pass spin forming schemes

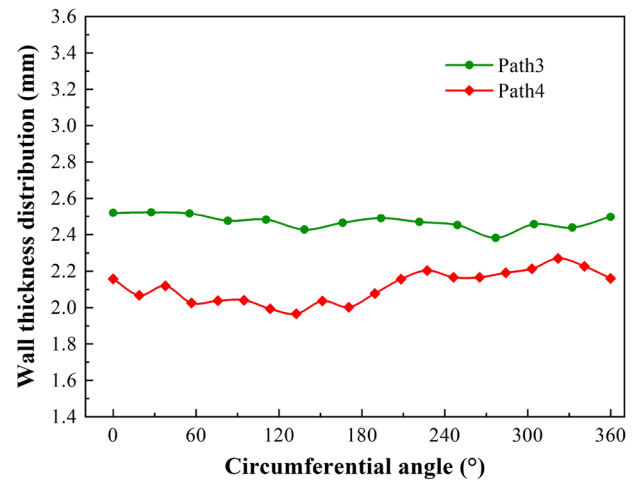


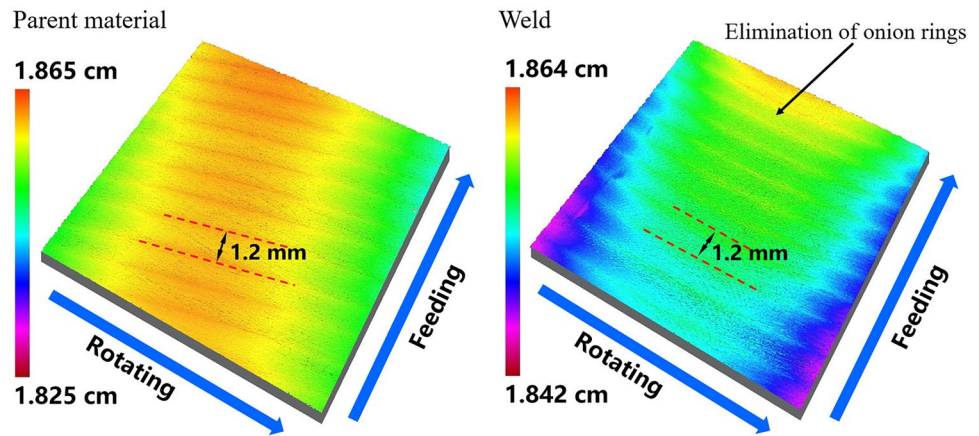
**Fig. 12** Wall thickness distribution



**Table 5** Forming results of spun components under four spin roller path schemes

Index	Roller path scheme			
	Single-pass	Two-pass	Three-pass	Eight-pass
Height (mm)	123.7	129.7	132	145.7
Unfitability (mm)	3.4	2	2.3	0.09
Spinning corrugations spacings (mm)	2.3	2.3	2.1	1.2
Roughness of parent material (μm)/longitude direction	3.25	2.85	2.43	2.26
Roughness of parent material (μm)/latitude direction	2.62	2.45	1.99	1.99
Roughness of weld (μm)/longitude direction	2.25	2.46	2.43	2.24
Roughness of weld (μm)/latitude direction	2.27	2.34	2.10	1.92

**Fig. 13** Surface topography of parent material and welds



### 5 Conclusions

In this study, three spin roller path schemes were firstly designed and assessed for the ability to manufacture thin-walled complex-curved-surface components from 2195 Al-Li alloy tailor-welded blanks. Since none of these three schemes can meet the geometrical requirements of the component, an improved spin roller path scheme was proposed and based on which the ideal spun component was successfully obtained. The following conclusions can be drawn:

1. With the increase of spin passes from one to three, the surface quality is significantly improved, and the component height gradually increases which approaches the ideal value. However, the corresponding open diameter diverges from the target value due to the unfitability.
2. After spin forming of tailor welded blanks, a deflection phenomenon of the welds was observed, and the deflection direction followed the mandrel rotating direction. The deflection angle increases gradually with the increase of spin passes.
3. A new eight-pass spin roller path scheme was proposed aiming to solve the unfitability problem near the open end and to improve the overall forming quality. The

forming height achieved 145.7 mm with an increase of 18%, while the unfitability value was reduced to 0.09 mm with a reduction of 97% compared to the other three schemes. In addition, both the wall thickness homogeneity and surface roughness were improved as well.

**Author contribution** HZ: conceptualization, investigation, software, methodology, experiments, formal analysis, writing — original draft. MZ: writing — review and editing, project administration, funding acquisition. ZZ: conceptualization, supervision, resources, writing — review and editing. RL: software. FM: data curation. XC: investigation. SC: data curation. YL: experiments.

**Funding** This work was supported by the National Science Fund for Distinguished Young Scholars of China (Project 51625505), the National Key R&D Program of China (Project 2020YFA0711100), the National Natural Science Foundation of China (Project 91860130, Project U1937203 and Project U1910213), and the Natural Science Basic Research Plan in Shaanxi Province of China (No. 2020JQ-166).

### Declarations

**Ethical approval** Not applicable.

**Consent to participate** Not applicable.

**Consent for publication** All authors have read and agreed to the published version of the manuscript.

**Competing interests** The authors declare no competing interests.

## References

- Xia QX, Xiao GF, Long H, Cheng XQ, Sheng XF (2014) A review of process advancement of novel metal spinning. *Int J Mach Tools Manuf* 85:100–121
- Gao PF, Yan XG, Li FG, Zhan M, Ma F, Fu MW (2022) Deformation mode and wall thickness variation in conventional spinning of metal sheets. *Int J Mach Tools Manuf*. 173:103846.
- Russo Iacopo M, Cleaver Christopher J, Allwood Julian M, Loukaides Eviropides G (2020) The influence of part asymmetry on the achievable forming height in multipass spinning. *J Mater Process Technol* 275:116350
- Wang L, Long H (2011) A study of effects of roller path profiles on tool forces and part wall thickness variation in conventional metal spinning. *J Mater Process Technol* 211(12):2140–2151
- Mohebbi MS, Rahimi Pour M (2019) Effects of temperature, initial conditions, and roller path on hot spinnability of AZ31 alloy. *Int J Adv Manuf Technol* 103:377–388
- Wu TC, Zhan M, Gu CG, Jiang HB, Yang H (2011) Quality analysis of first pass spinning of large complex thin-walled shell. *Mater Sci Technol* 19(01):121–126 (in Chinese)
- Wu TC, Zhan M, Jiang HB, Gu CG, Yang H (2011) Exploring effects of spinning gap on forming quality of second pass spinning of large-sized complicated thin-walled shell. *J Northwest Polytech Univ* 29(01):74–81 (in Chinese)
- Wei ZC, Li WD, Wan M, Xu CX, Huang ZB, Liu J (2010) Influence of roller-trace on multi-pass conventional spinning process. *Journal of Plasticity Engineering* 17(03):108–112 (in Chinese)
- Su P, Wei ZC (2014) Roller trace design and impact on outcome of spin forming molding. *Ordnance Industry Automation* 33(08):31–35+38 (in Chinese)
- Gan T, Kong QS, Yong ZQ, Zhao YX, Lai XM (2016) A numerical study of multi-pass design based on Bezier curve in conventional spinning of spherical components. *MATEC Web of Conferences* 80:15012
- Gan T, Yong ZQ, Zhao YX, Evsyukov SA, Lai XM (2018) Effects of backward path parameters on formability in conventional spinning of aluminum hemispherical parts. *Trans Nonferrous Met Soc* 28(2):328–339
- Li Y, Wang J, Lu GD, Pan GJ (2014) A numerical study of the effects of roller paths on dimensional precision in die-less spinning of sheet metal. *J Zhejiang Univ Sci A* 15(6):432–446
- Katiyar BS, Panda SK, Saha P (2020) Quasi-static crushing behavior of stretch formed domes of laser welded tailored blanks. *Thin Wall Struc* 107288
- Liu J, Wang AL, Gao HX, Gandra J, Zhan LH, Wang LL (2018) Transition of failure mode in hot stamping of AA6082 tailor welded blanks. *J Mater Process Technol* 257:33–44
- Parente M, Safdarian R, Santos AD, Loureiro A, Vilaca P, Natal Jorge RM (2016) A study on the formability of aluminum tailor welded blanks produced by friction stir welding. *Int J Adv Manuf Technol* 83(9–12):2129–2141
- Kinsey B, Liu ZH, Cao J (2000) A novel forming technology for tailor-welded blanks. *J Mater Process Technol* 99:145–153
- Khan A, Satya Suresh VVN, Regalla SP (2014) Effect of thickness ratio on weld line displacement in deep drawing of aluminium steel tailor welded blanks. *Procedia Mater Sci* 6:401–408
- Zadpoor AA, Sinke J, Benedictus R (2013) Experimental and numerical study of machined aluminum tailor-made blanks. *J Mater Process Technol* 200(1):288–299
- Silva MB, Skjoedt M, Vilaca P, Bay N, Martins PAF (2009) Single point incremental forming of tailored blanks produced by friction stir welding. *J Mater Process Technol* 209(2):811–820
- Bhagwan AV, Kridli GT, Friedman PA (2004) Formability improvement in aluminum tailor-welded blanks via material combinations. *J Manuf Process* 6(2):134–140
- Moayed H, Darabi R, Ghabussi A, Habibi M, Foong LK (2020) Weld orientation effects on the formability of tailor welded thin steel sheets. *Thin Wall Struc* 149(4):106669
- Ma F, Gao PF, Ma PY, Zhan M (2019) Power spinning of the curved head with tailor welded aluminum alloy blank: deformation, microstructure, and property. *Metals* 9(12):1359

**Publisher's Note** Springer Nature remains neutral with regard to jurisdictional claims in published maps and institutional affiliations.